Article

Hybrid of Angular and Distance Protection for Coexistence of 5G Base Stations and Satellite Earth Stations

Shuzhi Liu [1], **Yiqiao Wei** [1,2] **and Seung-Hoon Hwang** [1,*]

1   Division of Electronics and Electrical Engineering, Dongguk University, Seoul 04620, Korea;
    shuzhiliu@dongguk.edu (S.L.); weiyiqiao@cmsr.chinamobile.com (Y.W.)
2   China Mobile (Shanghai) Industrial Research Institute, Shanghai 200120, China
*   Correspondence: shwang@dongguk.edu; Tel.: +82-2-2260-3994

Abstract: In this study, we investigated the coexistence of the 5G communication network with a fixed-satellite service (FSS) in the 3.5 GHz and 26 GHz frequency bands. We analyzed an angular protection scheme for the FSS Earth station (ES) and 5G base stations (BSs). In addition, we defined the fixed BS-ES relative location, relative distance, and angular changes. The angular protection was integrated into the exclusion and restricted zones proposed by the distance protection scheme for simulation analysis to develop a transmit power control scheme based on the Citizens Broadband Radio Service. Its performances were extensively analyzed through simulations. The proposed scheme was evaluated in practical scenarios: rural macrocells, urban macrocells, and urban microcells, as defined by the 3rd Generation Partnership Project (3GPP). The influence of antenna type was also researched, and BSs with 4×4, 8×8 and 16×16 antenna arrays, as specified by 3GPP, were considered for 5G networks. Finally, the results prove that the angular protection solution can solve the coexistence of the 5G system and the FSS. In addition, when angular protection and distance protection are used simultaneously, the coexistence effect of the two systems can be strengthened. Moreover, this work provides a quantitative perception for selecting system parameters, including an interference margin for the different scenarios and antenna types, the exclusion size, and the reduction area.

Keywords: 5G system; fixed-satellite systems; coexistence/sharing scheme; angular protection

1. Introduction

The demand for 5G radio frequency (RF) communication systems is increasing. As a fifth-generation technology standard for broadband cellular networks, 5G has higher data rates, shorter delays, and more connections than 4G. In addition, 5G uses high, medium, and low frequencies [1]. Therefore, 5G can exploit specific characteristics of different frequency bands based on the application. For instance, low frequencies (below 2 GHz) extend the 5G mobile broadband to broad areas and deep indoor environments. High frequencies (above 6 GHz) provide additional capacity while delivering extremely high data rates, primarily required by 5G enhanced mobile broadband applications. Medium frequencies (2–6 GHz) manage the tradeoff between extended coverage and high capacity.

In 2018, the Republic of Korea conducted an auction of the 5G frequency bands, namely the 3.42–3.70 GHz and 26.5–28.9 GHz bands, as illustrated in Figure 1 [1]. In the future, additional frequencies may be allocated from the adjacent frequency bands. However, incumbent users exist in the existing bands, such as the fixed-satellite service (FSS) [2,3], intersatellite service, Earth-exploration satellite service, and meteorological satellite service [4]. The UK's communications regulator (Ofcom) identified the 3.8–4.2 GHz band as having the potential for increased sharing and developed proposals to ease the shared-frequency access in this band. The United States Federal Communications Commission (FCC) adopted a Notice of Proposed Rulemaking to release the 3.7–4.2 GHz band for new

wireless services while accommodating incumbents. In addition, the FCC sought comments on proposals, in order to promote a more spectrum-efficient, intensive, and fixed use of the band on a shared basis. Several GSM studies have addressed the access to the current utilization of the C-band (3.5–4.2 GHz). These studies defined a strategy and roadmap to release this band to support the deployment of 5G services [5].
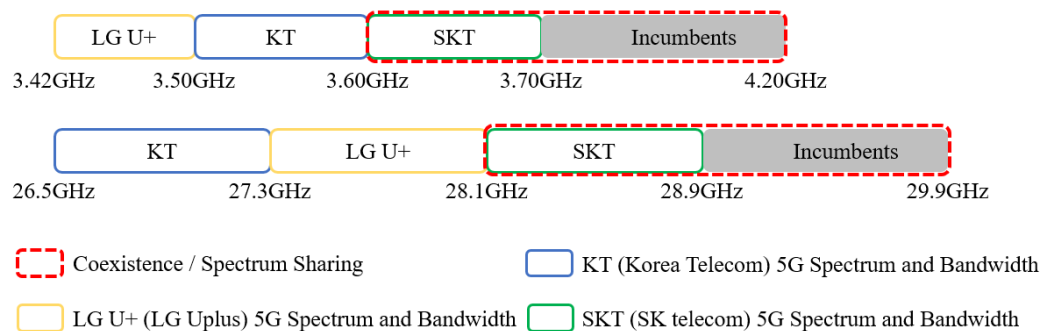

Figure 1. Korea's 5G frequency allocations and adjacent bands [1].

Interference is the primary problem of the coexistence of two communication systems on one frequency band. Four types of interference exist between 5G and FSS systems: from the 5G base station (BS) to the FSS earth station (ES), from 5G users to the FSS ES, from FSS devices to the 5G BS, and from FSS devices to 5G users. In this study, we followed previous research [6] and focused on minimizing the interference of BS to ES and achieving the coexistence of FSS and 5G BS.

In previous studies, refs. [7,8] confirmed that distance protection schemes can effectively solve the problems caused by interference. As part of the Citizens Broadband Radio Service (CBRS) development, we suggested a distance protection strategy for FSS ESs and 5G BSs [6]. The suggested method was evaluated against three real scenarios of rural macrocells (RMa), urban macrocells (UMa), and urban microcells (UMi), the size of the exclusion zone is different for various scenarios (RMa > UMa > UMi), where higher elevation angles imply larger off-boresight angles. Antenna arrays offer a wider confined area on the ES's north side than omnidirectional antennas. Increasing the number of antenna components also solves the problem of reducing the restricted region caused by directional attenuation. When the antenna array is employed in the urban scenario (UMa and UMi), the average Tx power reduction is minimal since many cells can only cut their Tx power by 1 dB. If the Tx power is lowered by 1 dB, and most BSs must further reduce Tx power when using an omnidirectional antenna. When using antenna arrays in UMa and UMi, the proposed power control strategy is more effective. It was found that the influence of ES/BS-related angles on frequency band coexistence was not studied in prior studies.

In the study of [9], the distance protection scheme was incorporated into the analysis of the protection band and the angle of arrival to achieve the coexistence of LTE-Advanced and FSS services. Therefore, we propose an angular protection scheme to solve the influence of the ES antenna elevation angle on the protection mode. The angle protection was integrated into the exclusion and restricted zones proposed by the distance protection scheme for simulation analysis. Finally, in restricted areas, some interactive power control schemes inspired by the power control scheme used in CBRS were proposed and evaluated. The contributions of this article are summarized as follows:

- The fixed BS-ES relative location, BS-ES relative distance, and angle changes illustrate the principle of angular protection from the easier to the more advanced cases;
- Shutting off the harmful beam was performed to decrease the exclusion and restriction zones, and to reduce the BS TX power in the restriction zone for angular protection. Three types of beam shut-off were investigated to demonstrate the tradeoff between the BS coverage and the coexistence of ES protection;

- The distance protection approach of the literature was used, and the combination of angular protection and distance protection was evaluated. In addition, the efficiency of the angular protection and the combination of angular protection and distance protection, were evaluated and compared. Four beam shut-off ranges (45°, 90°, 180° and 270°) were investigated regarding the tradeoff between the BS beam sweep and the coexistence of ES protection.

The remainder of this study is organized as follows. The related work, basic scenarios, simulation parameters, and interference derivations are presented in Section 2. The angular protection methods and combination with the distance protection scheme are detailed in Section 3. The experimental results obtained using the proposed method are presented and discussed in Section 4. Finally, the conclusions are drawn, and perspectives are provided in Section 5.

2. The Related Work

2.1. Comparison of Space Domain and Angular Domain in Exclusion Zones

Existing efforts focuses on releasing new frequency bands to allow 5G deployment. Two methods were proposed in [10] to enable administrations to protect existing users in the 3.6–3.8 GHz band while allowing mobile/fixed communication networks to use them as new entrants. The authors of ref. [11] investigated several BS/ES deployment plans, antenna configurations, and transmitter parameters to explore the millimeter wave frequency spectrum and the coexistence of cellular and satellite services. Techniques for reducing passive interference are often used in contemporary coexistence strategies. Most coexistence studies use the space domain technique. It is further separated into exclusion zones and restriction zones, according to the definition of [11], an exclusion zone is a geographical area within which licensees are not allowed to have active radio transmitters, and restriction zones are geographical areas within which victim receivers will not be subject to harmful interference caused by interferer transmissions. The space domain is based on the interference/noise (I/N) protection threshold technique, involving a maximum permitted interference at the input to the FSS ES [2,11–14].

The restriction zones and BS transmit (Tx) power control schemes were also studied through the distance protection method. The advantages of this scheme are its simple layout, high coexistence efficiency, and adaptability to several environments. In the angular domain with the exclusion zone protection method, the BS can shut off the aligned beams, so that the beams can reach the angular exclusion range (i.e., the beam direction, the BS to ES direction is less than the angular protection threshold). A protection angle can be paired with zone protection to reduce the protection radius in dense and angular areas [2]. This scheme is advantageous in terms of being unrestricted on the space domain. A comparison of the two methods is shown in Table 1.

Table 1. Advantages and disadvantages of using various protection methods.

	Space Domain Exclusion Zones	Angular Domain Exclusion Zones
Advantage	Simple and effective	No/less restricted on the space domain
Disadvantage	Network coverage dead zones Restricts 5G deployment	Advanced antenna is required to generate a directional beam Increases the cost and complexity of the system

2.2. Basic Scenarios and Parameters Setting

In the previous work [6], we confirmed that the antenna gain is related to the deviation of the azimuth and elevation angle from the boresight, and we proposed a plan to protect the target. For the protection target, i.e., the FSS ES, the ES is assumed to be located at the center of the area with a coordinate of (0, 0). Further, the azimuthal orientation of the ES antenna is assumed to be true north, while the ES antenna elevation orientation, i.e., elevation angle, differs for various ESs, according to the ES deployment requirements. The cellular BS (eNodeB/gNodeB) was assumed to be deployed at any possible location (X, Y)

around the ES. Moreover, the plan assumed that the azimuth of the BS antenna was true south. The relationship between the positions of BS and FSS ES is shown in Figure 2.
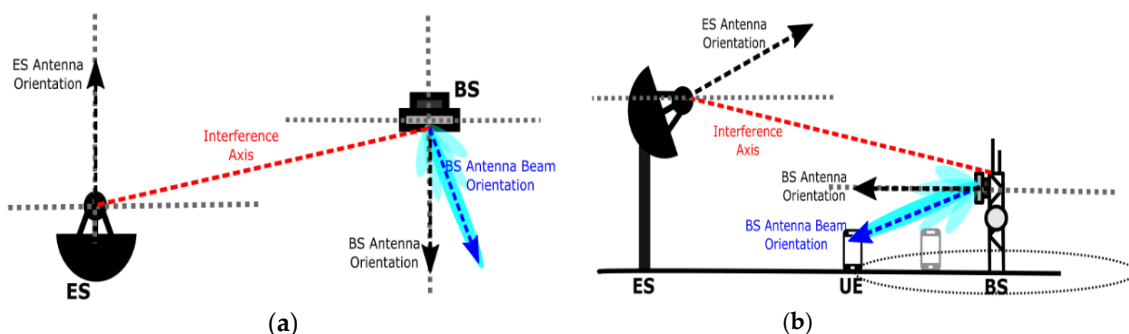

(a)   **(b)**

Figure 2. Carrier frequency set to the center frequency in the (**a**) azimuthal and (**b**) elevation planes [6].

During the simulation, we used a three-dimensional (3D) (X, Y, Z) coordinate system to present the results. In this coordinate system, the *x*- and *y*-axes represent the latitude and longitude coordinates of the BS, respectively, and the *z*-axis represents the target measurement value, such as the ES antenna gain, path loss, and I/N data. Three scenarios were considered in this study: RMa, UMa, and UMi [14]. The ES antenna heights and diameters, BS antenna heights, intersite distances, propagation losses, shadow fading, and LOS/nonline of sight (NLOS) probability distributions are different for each scenario. Furthermore, the carrier frequency was set to 3.95 GHz, which corresponds to the center frequency of the 3.7–4.3 GHz range. The FSS ES simulation parameters used in all considered scenarios are presented in Table 2.

Table 2. Fixed-satellite service (FSS) Earth station parameters [15–18].

Parameter	RMa	UMa	UMi	Parameter	RMa	UMa	UMi
ES antenna diameter (m)	10	2.4	2.4	Thermal noise (dBm/Hz)	−179	−179	−179
ES antenna pattern		ITU-R S.465-6		ES bandwidth (MHz)	36	36	36
ES antenna height (m)	7	30	30	ES antenna maximum gain (dBm)	56	56	56
BS antenna height (m)	35	25	10	BS channel bandwidth (MHz)	20	20	20
Intersite distance (m)	1732	500	200	LOS shadow fading (dB)	6	4	4
BS maximum Tx power (dBm)	46	38	38	NLOS shadow fading (dB)	8	6	7.82
Single antenna element in MIMO antenna array	8	8	8	BS minimum coupling loss (dB)	80	70	70

Notes: ES: Earth station; BS: base station; Tx: transmission; MIMO: multiple-input multiple-output; LOS: line of sight; NLOS: nonline of sight; RMa: rural macrocell; UMa: urban macrocell; UMi: urban microcell.

2.3. Interference Derivation

In the previous work, we focused on the interference calculation of the azimuth and elevation planes and provided the following formulas:

$$I_{FSS\ ES \to BS} = P_{BS\ tx} + G_{FSS\ ES} + G_{BS} - PL, \tag{1}$$

where $P_{BS\ tx}$ is the transmit station signal power density (in dBm/MHz) [19,20] and $G_{FSS\ ES}$ represents the antenna gain of the ES in the direction of the transmit station (in dBi) [8]. In addition, G_{BS} is the 5G BS antenna gain using massive MIMO antenna array in the direction of the ES to account for the beamforming antenna pattern (in dBi) [16,21]. Finally, PL represents the combined path loss from all the possible BS locations to the ES [16].

The cellular network simulation results in [6] demonstrate that the path loss in rural areas is always lower than that in urban areas (i.e., the path loss for RMa is slightly higher

than that for UMa and UMi). Research reveals that LOS and NLOS scenarios should be used together in a real environment, and NLOS paths are usually the main loss component in urban areas. In addition, by increasing the number of elements in the antenna array, the main lobe beam can provide higher gain while generating more side lobes. More elements in an antenna result in a narrower main lobe beam. In the scenario of a 16×16 antenna array, a smaller beam sweep angle provides a better gain effect. The gain effect with a beam sweep angle of $60°$ is 20% lower than that with a beam sweep angle of $0°$. According to [19,20], a Tx power limit of 38 dBm was selected for the mid-range BS, whereas the wide-area BS does not consider the upper limit. Moreover, the UMa and UMi also selected the mid-range BS Tx power limit (38 dBm), whereas the RMa scene in the wide-area BS selected the 46 dBm limit, based on the defined maximum macrocell BS Tx power [17].

3. Angular Protection Methods

This section addresses the fixed BS-ES relative location, BS-ES relative distance changes, and BS-ES relative angle changes to illustrate the principle of angular protection in both easy and advanced cases. Finally, the combinations of the distance protection and angular protection methods (i.e., the exclusion zone, restriction zone, and angular protection method) were analyzed.

3.1. Angular Protection: Fixed BS-ES Relative Location

In the fixed BS-ES relative location technique, the following assumptions were made:

- There is a fixed BS location true north of the ES and 15 km away from the ES;
- There is a fixed $0°$ azimuth angle of the BS regarding the ES ($\varphi = 0$);
- The steering beam of the antenna array (φ_s) changes from $-180°$ to $180°$ with a step size of 1.

The BS interference was calculated in each step to compute the beam shut-off angle φ_{off} (i.e., the size of the beam angle that must be shut off). If the interference with the current beam sweep angle φ_s is higher than the I/N interference threshold, this beam angle must be shut off to protect the ES. The beam shut-off angle φ_{off} increases by $1°$, as presented in Figure 3.
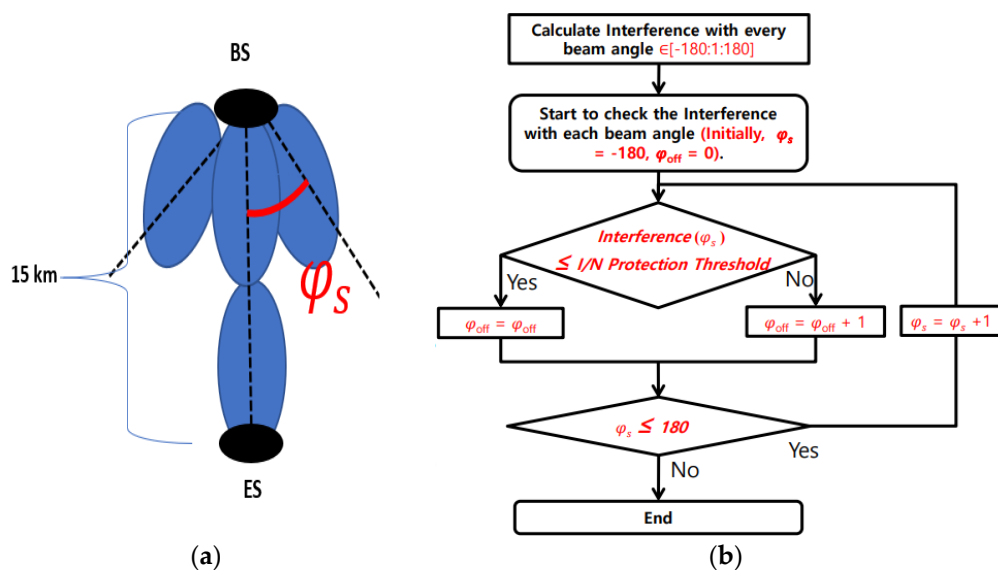
Figure 3. Fixed base station to Earth station: (**a**) relative azimuth and (**b**) flux gram.

To compute the interference of each beam angle, the range of was set to [180:1:180]. The parameters of the two interferences ($\varphi_s = 180$, $\varphi_{off} = 0$) were verified and initialized before the computation. The next stage was to assess the interference. If interference φ_s is less than or equal to the I/N protection threshold parameter, φ_{off} is assigned to φ_{off};

if interference φ_s is more than the I/N protection threshold parameter, φ_{off} is specified to rise by 1°. A second judgment on φ_s is required next. Iteratively 1 can be added to the initial value of φ_s until φ_s is larger than 180°, finishing the operation and generating the interference φ_s and φ_{off}.

Figure 4 depicts the I/N from the BS to the ES for a distance of 15 km with a 4 × 4 antenna array, regarding the sweep angle RMa LOS, sweep angle UMa LOS, and sweep angle UMi LOS, respectively. Figure 5 presents the corresponding beam angle needed to be shut off, using a more intuitive illustration. The angle in the red area is the shut-off beam. It corresponds to the beam angle, which provides a higher I/N than the red line in Figure 4. The interference protection criterion was assumed as the threshold of interference-to-noise ratio (I/N) of −12.2 dB (red line in Figure 4) was derived from [22]. The sweep angle, which provides a higher interference than the −12.2 dB threshold, should be shut off. The beam shut-off range is higher for the LOS than for the NLOS because of the lower path loss, as displayed in Figure 5. Hence, the I/N values are higher for the LOS for all beam directions. Thus, more beam angles must be shut off. For the UMi NLOS, no beam angle must be shut off because the interference of all beam angles is lower than the I/N threshold.
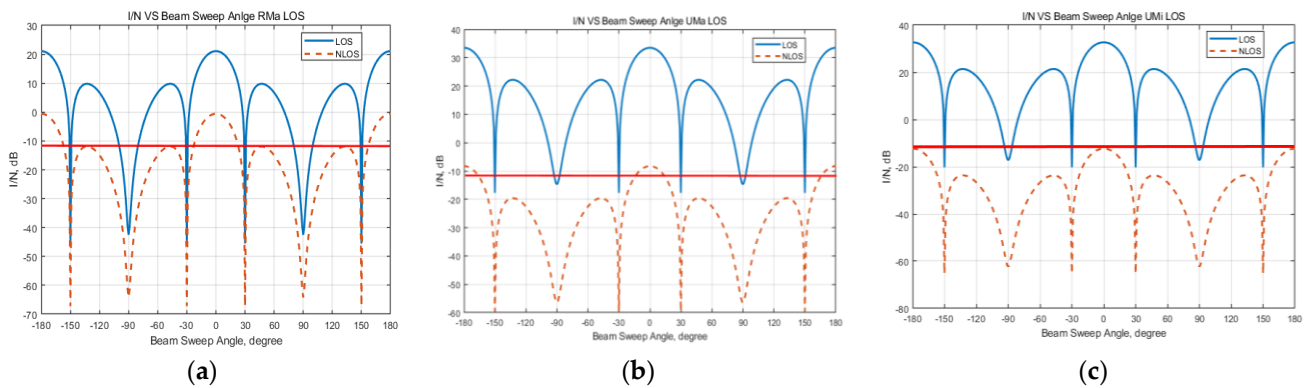

Figure 4. Interference/noise (I/N) from the base station (BS) to the Earth station (ES) for a distance of 15 km with a 4 × 4 antenna array. (**a**) Rural macrocell; (**b**) urban macrocell; (**c**) urban microcell.
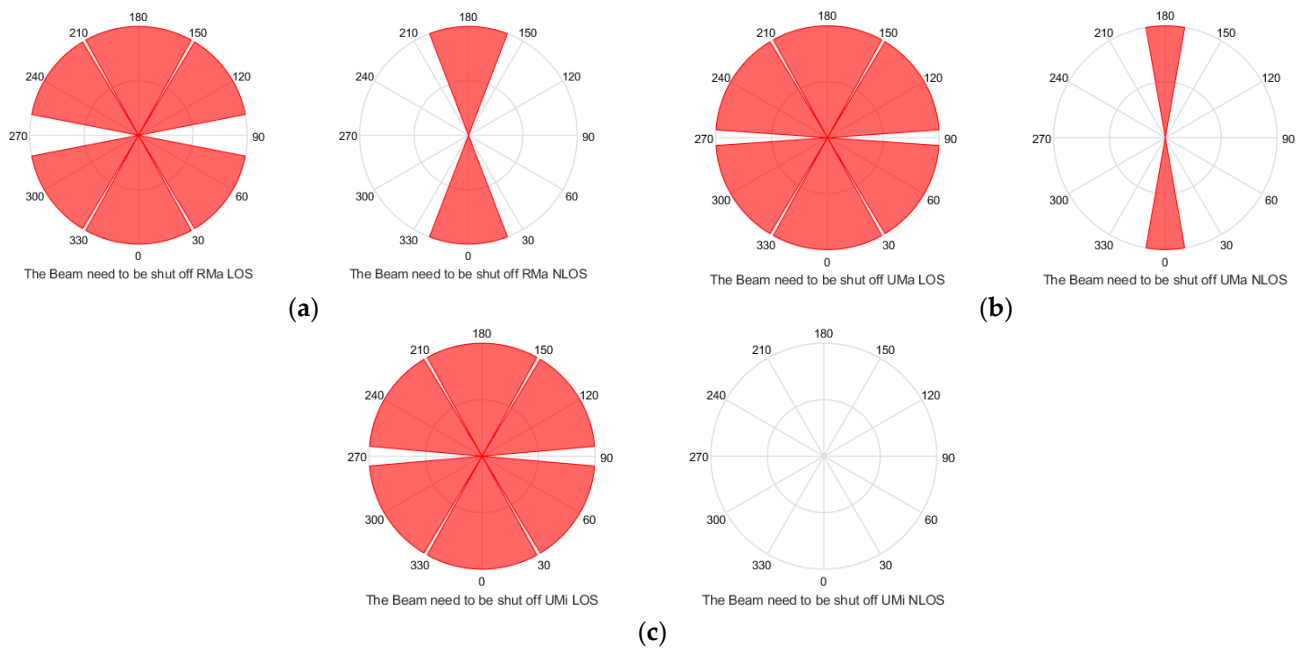

Figure 5. Beam angles that should be shut off: RMa (**a**), UMa (**b**) and UMi (**c**) LOS and NLOS.

3.2. Angular Protection: BS-ES Relative Distance Changes

The following assumptions were made for the BS-ES relative distance changes:

- The ES location is fixed while the distance between the BS and ES varies between 1 m and 20 km;
- There is a fixed 0° azimuth angle of the BS regarding the ES ($\varphi = 0$);
- The steering beam of the antenna array (φ_s) varies between −180° and 180°;
- The interference of the BS when the beam directs to all possible directions was evaluated;
- The beam sweep angle φ_s, which has a frequency higher than the I/N interference threshold, should be considered for shut-off.

Figure 6 presents the BS-ES relative change distance. In this case, the azimuth angle of the BS about the ES remains unchanged, whereas the distance between the ES and BS varies from 1 km to 20 km. The interference calculation process follows the structure shown in Figure 3b. Figure 7 illustrates the beam shut-off angle, concerning the BS-ES distance, using an ES antenna elevation distance of 0 to 20 km and a 4 × 4 antenna array. The LOS and NLOS cases were separated to better illustrate the principle. The beam shut-off angle becomes smaller as the distance between the BS and ES increases. A longer distance implies a higher path loss and lower interference for all beam angles, which results in a need to shut off fewer beam angles. For NLOS, with the same BS-ES distance, the beam shut-off angle for the three cases is RMa > UMa > UMi. As for LOS, with the same BS-ES distance, the beam shut-off angle for the three cases is RMa <UMa < UMi.
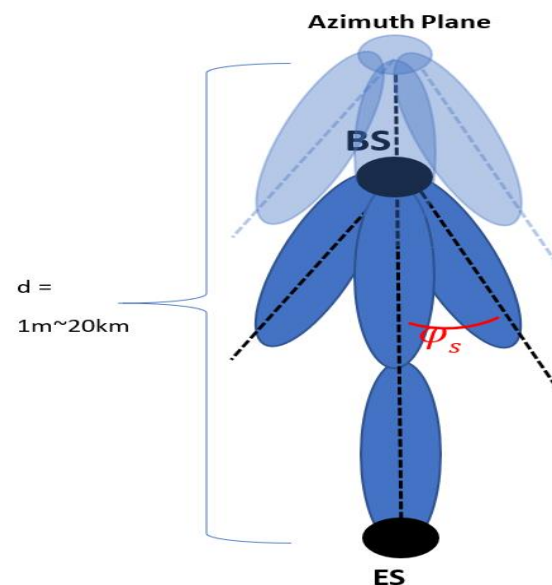
Figure 6. BS-ES relative distance change.

3.3. Angular Protection: BS-ES Relative Angle Changes

The following assumptions were made for the BS-ES relative angle changes:

- The ES location is fixed, whereas the distance between the BS and ES is 15 km;
- The BS moves in a circle around the ES (i.e., the azimuth angle of the BS about the ES (φ) varies between −180° and 180°);
- The steering beam of the antenna array (φ_s) varies between −180° and 180°;
- The BS interference when the beam directs to all possible directions was evaluated;
- The beam sweep angle φ_s, which has a higher frequency than the I/N interference threshold, should be considered for shut-off.

Figure 7. Beam shut-off angle vs. BS-ES distance (ES antenna elevation distance of 0 to 20 km and a 4 × 4 antenna array).
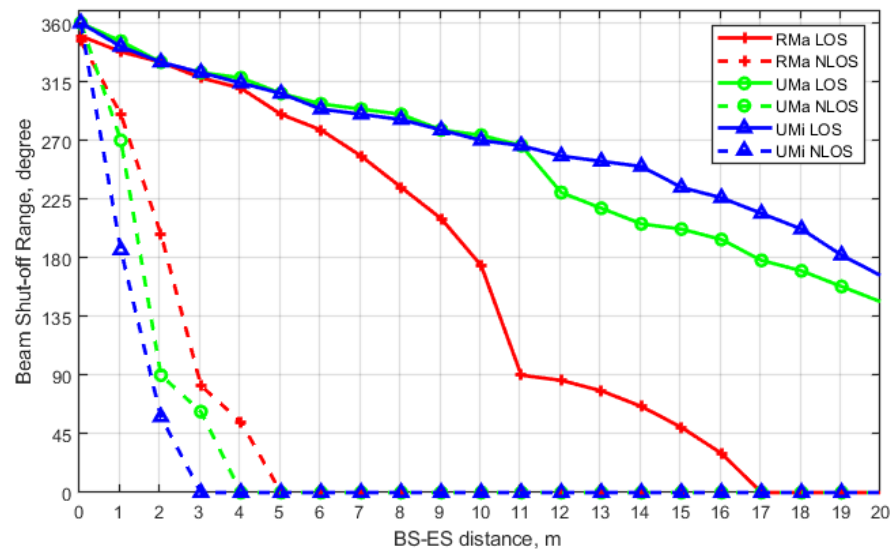
Figure 8 presents the BS-ES relative change angle. The distance between the ES and BS was kept at a fixed 15 km in this case, but the azimuth angle of the BS about the ES changed from −180° to 180°. The calculation process of interference follows the structure in Figure 3b.
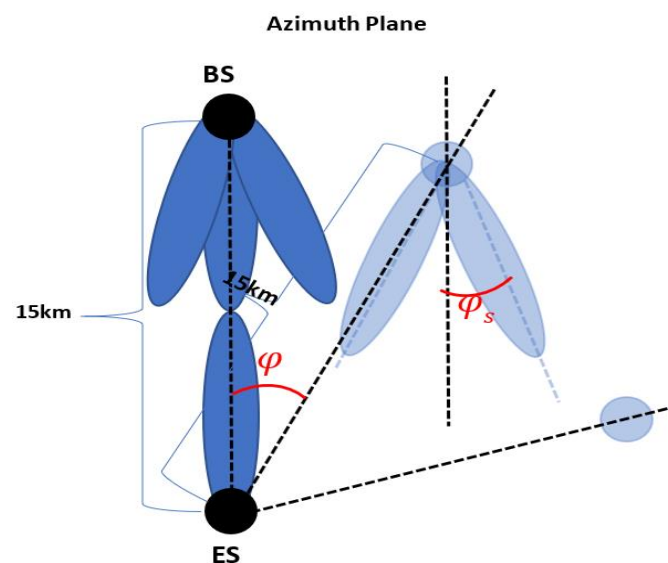
Figure 8. BS-ES relative angle change.

With an ES antenna elevation angle between -180° and 180°, a distance of 15 km, and a 4 × 4 antenna array, Figure 9 depicts the beam shut-off angle. The LOS and NLOS instances were presented separately in order to better demonstrate the concept. As the absolute BS-ES angle rises, the range of the beam shut-off angle decreases proportionally. In the presence of a greater absolute BS-ES angle, there is a higher antenna gain attenuation, resulting in reduced interference for all beam angles and the requirement to turn off fewer beam angles overall. The beam shut-off angle for NLOS with the same BS-ES distance is RMa > Uma > UMi for the three scenarios of the same BS-ES distance. Using the same BS-ES distance for all three situations, the beam shut-off angle for LOS is RMa < Uma ≈ UMi. for all three cases.

Figure 9. Beam shut-off angle vs. BS-ES angle (ES antenna elevation angle = $-180°$ to $180°$, $d = 15$ km, 4×4 antenna array).

3.4. Angular Protection with Distance Protection

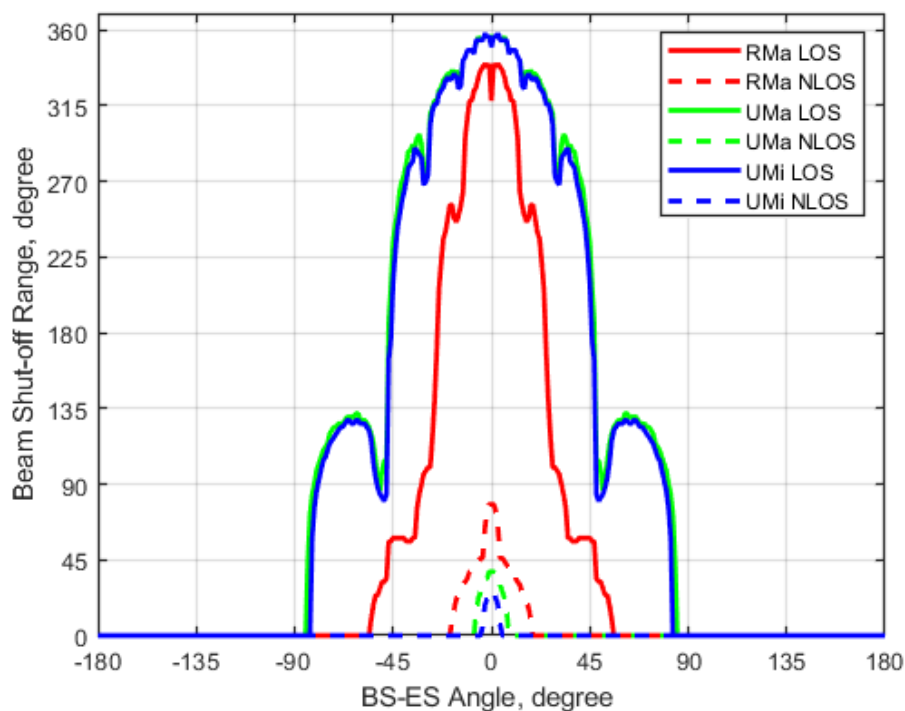In our previous work, we proposed a coexistence scheme for distance protection and defined the exclusion and restriction zones. However, this solution does not consider the influence of angles on the coexistence of frequency bands. Therefore, we integrated the angle protection scheme proposed in this work based on the original distance protection scheme. Further, based on the exclusion and restriction zones, the significance of the angle protection scheme for the coexistence of frequency bands was analyzed. The following assumptions were made in this section:

- The ES location is fixed, whereas the distance between the BS and ES is 15 km;
- The BS moves in a circle around the ES (i.e., the azimuth angle of the BS regarding the ES (φ));
- Both the BS-ES angle and BS-ES distance change with the BS (x, y);
- The steering beam of the antenna array (φ_s) varies between $-180°$ and $180°$.

Figure 10 illustrates the (a) angular protection and (b) flux gram of the combination of the exclusion and restriction zones. Both the BS-ES angle and BS-ES distance change with (x, y). Therefore, the beam shut-off angle φ_{off} also changes with the BS coordinates, as depicted in Figure 8. When calculating the result $\varphi_{off}(x, y)$ of the beam shut-off angle φ_{off} and every BS location (x, y), the relationship between $\varphi_{off}(x, y)$ and the beam shut-off range was analyzed. Only $\varphi_{off}(x, y)$ is less than or equal to the beam shut-off range; thus, the BS can be deployed at the current location. Otherwise, it cannot be deployed. A predefined beam shut-off range exists (i.e., a threshold for the beam shut-off angle (φ_{off})).

This threshold represents how much beam angle we are willing to sacrifice, whereas a higher value corresponds to a higher level of angular protection. The four predefined beam shut-off ranges ($45°$, $90°$, $180°$ and $270°$) were investigated to demonstrate the tradeoff between the BS coverage and the coexistence of ES protection. Although the angle of $270°$ was turned off, it was also included in the investigation to illustrate the upper limit of angular protection. More precisely, sacrificing 75% of coverage of the BS makes this range not worth deploying. The derivation of the restriction zone under different beam shut-off ranges leads to the same analysis conclusions.
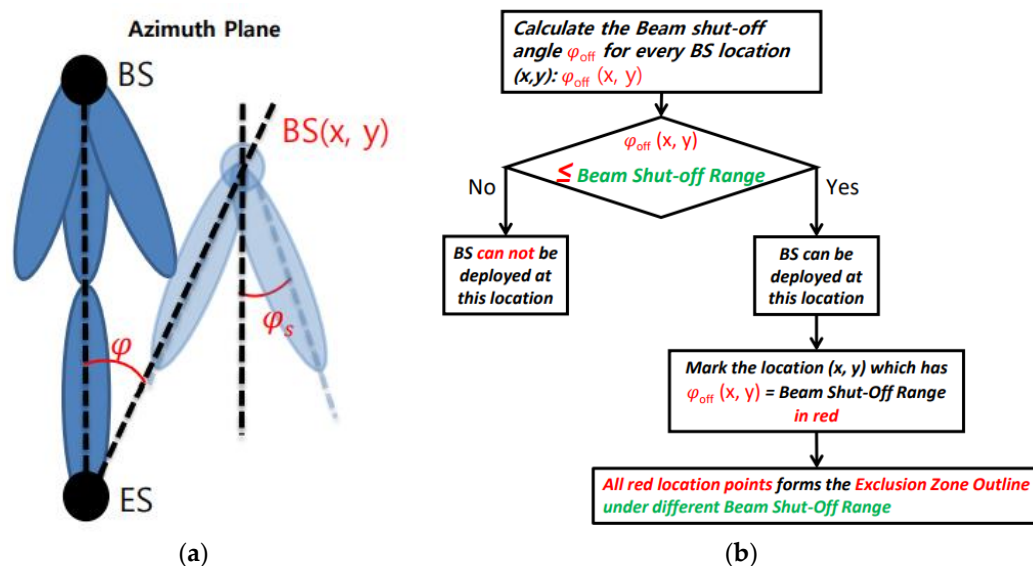
Figure 10. Combination of the exclusion and restriction zones: (**a**) angular protection and (**b**) flux gram.

4. Numerical Results

4.1. Angular Protection with Distance Protection: Exclusion Zone

Figure 11 presents the reduction in the exclusion zone when using the proposed angular protection where different antenna types are involved with RMa (a), UMa (b), and UMi (c). A higher beam shut-off range implies a lower BS interference, leading to a smaller exclusion zone. For a 4×4 antenna array, when $45°$ beam angles are sacrificed, the size decrease is negligible. In contrast, when using 8×8 and 16×16 antenna arrays, the $45°$ beam angle shut-off leads to a significant decrease in the exclusion zone.

In addition, using a 16×16 antenna array leads to a higher exclusion zone decrease because the antenna array can steer a narrower beam when more elements are in the antenna array. Without angular protection, the exclusion zone of the 8×8 and 16×16 arrays are larger than that of the 4×4 array. However, when the beam shut-off range is $45°$, the exclusion zone of the 8×8 array 16×16 arrays become smaller than that of the 4×4 array. Therefore, when the antenna array has more elements, the angular protection becomes more effective. As for UMi, a minor improvement is achieved when using $90°$, $180°$ and $270°$ beam shut-off ranges, compared with the $45°$ beam shut-off range. Without angular protection, the exclusion zone of the 8×8 and 16×16 arrays are greater than that of the 4×4 array. However, when the beam shut-off range is set to $45°$ or higher, the exclusion zone of the 8×8 and 16×16 arrays become smaller than that of the 4×4 array. In conclusion, the advantage of increasing the number of elements in the antenna array in terms of angular protection efficiency is more significant for UMi than RMa. Finally, a higher beam shut-off range results in a lower BS interference, which leads to a smaller exclusion zone.
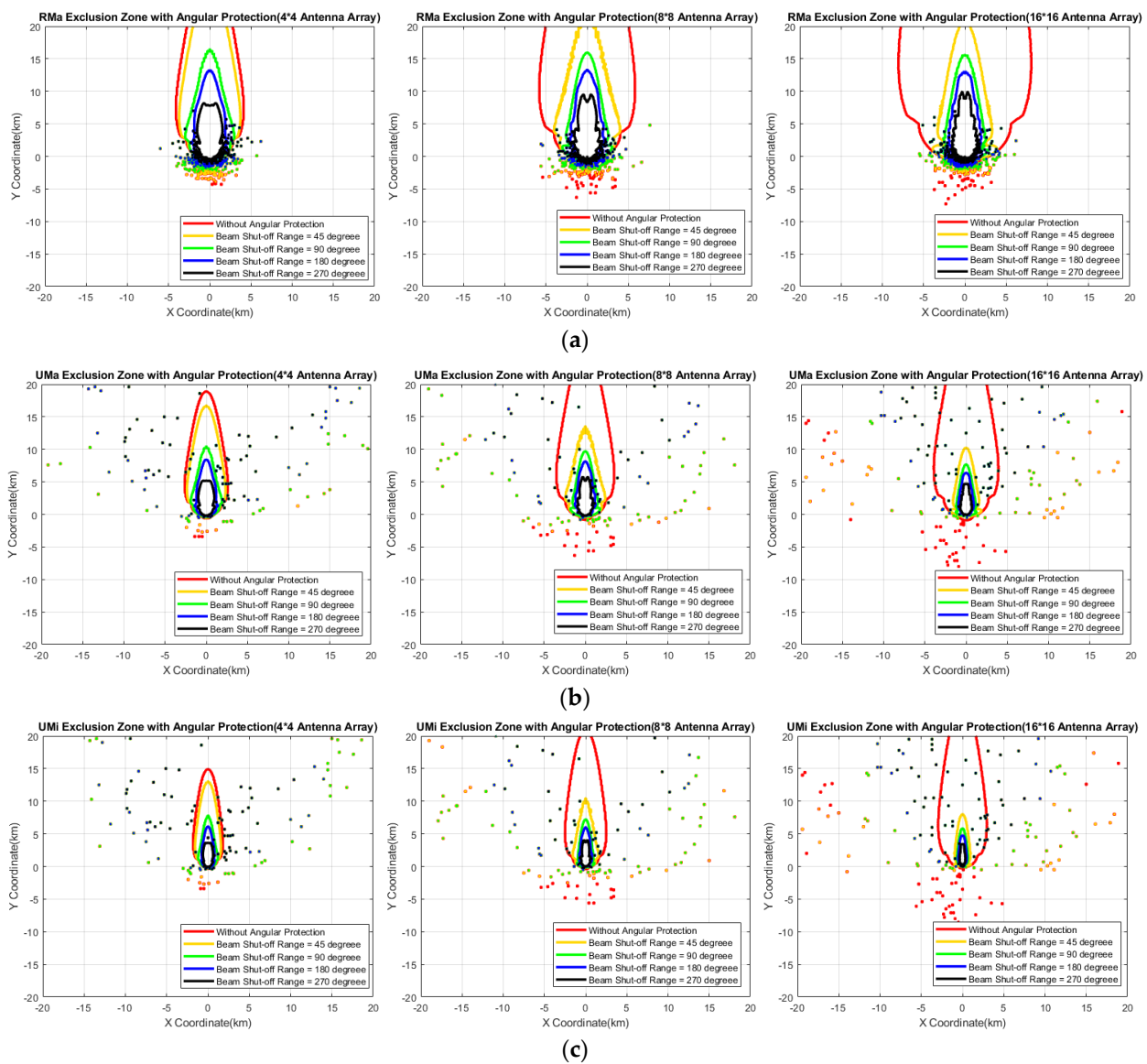
Figure 11. Reduction in the exclusion zone using the proposed angular protection for various antenna types. (**a**) Rural macrocell (RMa); (**b**) urban macrocell (UMa); (**c**) urban microcell (UMi).

4.2. Angular Protection with Distance Protection: Restriction Zone

Similar to the case of the exclusion zone with angular protection, more antenna array elements lead to more effective angular protection. Without angular protection, the restriction zone of the 8×8 and 16×16 arrays is larger than that of the 4×4 array. However, when the beam shut-off range is set to $45°$ or higher, the restriction zones of the 8×8 and 16×16 arrays become smaller than that of the 4×4 array.

Figure 12 illustrates the reduction in the restriction zone when using the proposed angular protection for various antenna array sizes in RMa, UMa, and UMi. A higher beam shut-off range results in lower BS interference, leading to a smaller restriction zone. In contrast to the exclusion zone, the size of the restriction zone keeps significantly decreasing as the beam shut-off range increases to $90°$, $180°$ and $270°$. The advantage of increasing the number of elements of an antenna array in terms of angular protection efficiency is more significant in UMi than RMa. Without angular protection, the zone of the 8×8 and 16×16 arrays are larger than that of the 4×4 array, as illustrated in Figure 12c. However, when the beam shut-off range is set to $45°$ or higher, the zone of the 8×8 and 16×16 arrays become smaller than that of the 4×4 array.
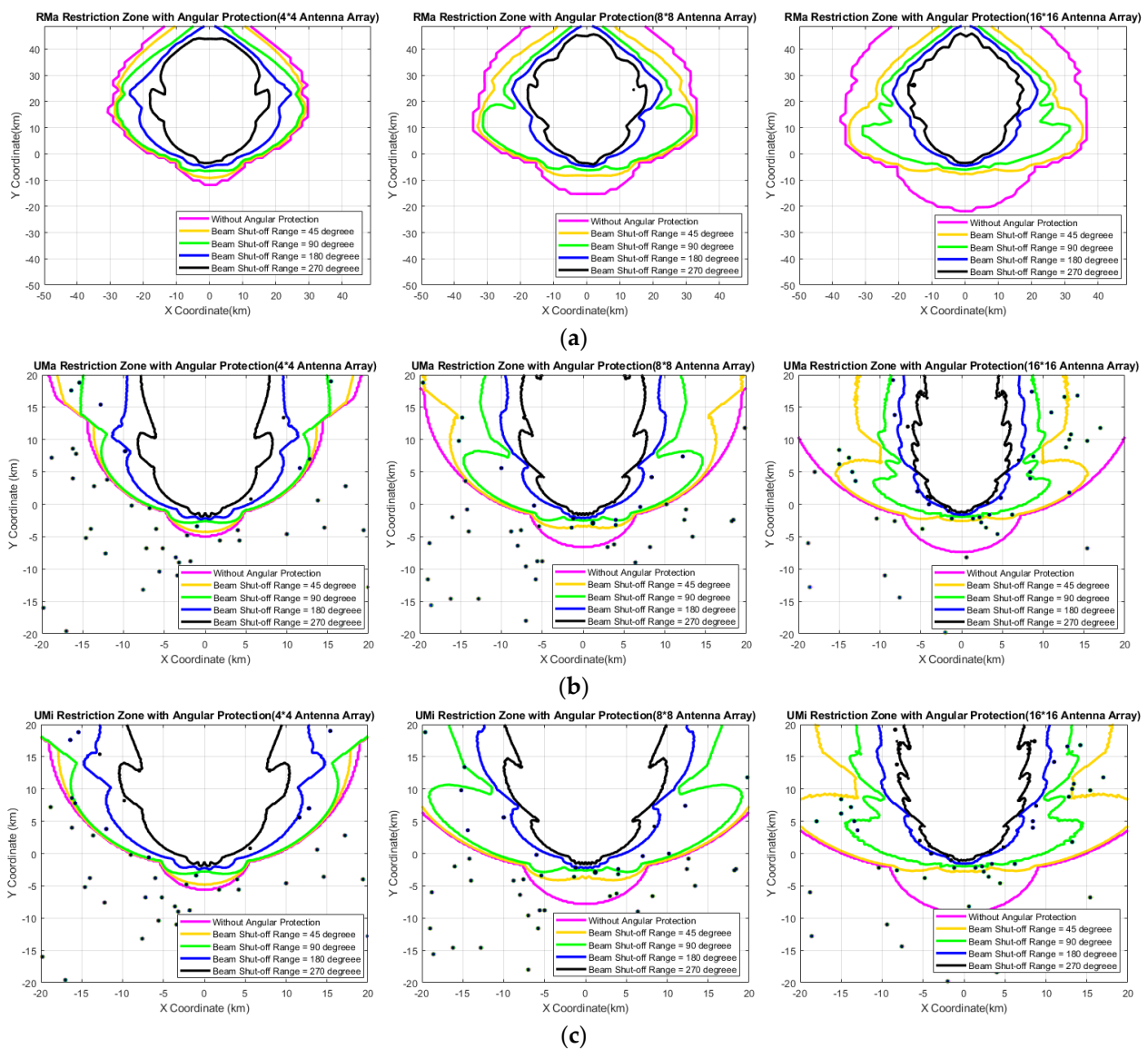
Figure 12. Restriction zone reduction using the proposed angular protection for antenna sizes in (**a**) RMa, (**b**) UMa, and (**c**) UMi. (**a**) Rural macrocell (RMa); (**b**) urban macrocell (UMa); (**c**) urban microcell (Umi).

For easier understanding of the results, we combined the exclusion zone figure, restriction zone figure and the data, as shown in Tables 3–5. Tables list the mean transmission (Tx) power reduction in the restriction zone for RMa, UMa, and UMi using 4×4, 8×8 and 16×16 antenna arrays, respectively. The number of deployable base stations was calculated by simulator based on [8], and there will be some base stations in restriction zone, this is the number of restriction zone base stations.

Using a higher beam shut-off range (sacrificing more beam angles) can bring following 3 kinds of affect, case 1 is a smaller exclusion zone that can increase the total number of BSs which can be deployed; case 2 is a smaller exclusion zone that can increase number of BSs in restriction zone; and case 3 is a smaller restriction zone that can decrease the number of BSs in the restriction zone. Therefore, the higher beam shut-off range can cause case 2 and case 3, which affect is the dominant will decide the increase or decrease in number of BSs in restriction zone.

The percentage of deployed BS requiring Tx power control depends on the ratio of the number of BSs in the restricted area to the total number of deployable BSs. The size change in Exclusion Zone and Restriction Zone will make BSs move into or move out

of the Restriction Zone. Some BSs provide relatively higher interference (BSs are closer to ES) and some of these BSs provide relatively low interference (BSs are farther from to ES). BSs that provide higher interference are required to decrease more Tx power in the proposed iterative power control scheme. This makes the mean Tx power reduction in restriction zone increase. Therefore, the percentages of BSs which provide different level of interference in number of BSs in Restriction Zone decide the change in mean Tx power reduction in restriction zone.

Table 3. Mean transmission (Tx) power reduction in the restriction zone for RMa, UMa, and UMi, using a 4×4 antenna array.

Region Type	Beam Shut-Off Range	No. of Deployable Base Stations	Restriction Zone Interference Threshold	No. of Restriction Zone Base Stations	% Deployed Base Stations Requiring Tx Power Control	Mean Tx Power Reduction in Restriction Zone
RMa (100 km $\times$ 100 km)	No Protection	3302	-47.39 dB	606	18.35%	14.30 dB
	45°	3316	-47.41 dB	590	17.79%	15.15 dB
	90°	3345	-47.44 dB	523	15.64%	12.52 dB
	180°	3350	-47.45 dB	390	11.64%	11.97 dB
	270°	3356	-47.46 dB	279	8.31%	9.32 dB
UMa (30 km $\times$ 30 km)	No Protection	3463	-47.59 dB	1450	41.87%	19.64 dB
	45°	3503	-47.64 dB	1455	41.53%	20.55 dB
	90°	3624	-47.79 dB	1504	41.50%	19.26 dB
	180°	3654	-47.82 dB	1143	31.28%	18.65 dB
	270°	3686	-47.87 dB	809	21.95%	17.11 dB
UMi (30 km $\times$ 30 km)	No Protection	21,831	-55.59 dB	10,960	50.20%	26.79 dB
	45°	22,036	-55.63 dB	11,022	50.02%	27.74 dB
	90°	22,509	-55.72 dB	11,156	49.56%	25.02 dB
	180°	22,603	-55.74 dB	8910	39.41%	24.43 dB
	270°	22,697	-55.75 dB	6211	27.36%	22.34 dB

Table 4. Mean transmission (Tx) power reduction in the restriction zone for RMa, UMa, and UMi using an 8×8 antenna array.

Region Type	Beam Shut-Off Range	No. of Deployable Base Stations	Restriction Zone Interference Threshold	No. of Restriction Zone Base Stations	% of Deployed Base Stations Requiring Tx Power Control	Mean Tx Power Reduction in Restriction Zone
RMa (100 km $\times$ 100 km)	No Protection	3252	-47.32 dB	746	22.93%	15.84 dB
	45°	3325	-47.42 dB	674	20.27%	14.25 dB
	90°	3344	-47.44 dB	530	15.85%	12.80 dB
	180°	3351	-47.45 dB	366	10.92%	12.61 dB
	270°	3357	-47.46 dB	271	8.07%	9.59 dB
UMa (30 km $\times$ 30 km)	No Protection	3352	-47.45 dB	1682	50.18%	20.84 dB
	45°	3563	-47.72 dB	1803	50.60%	20.83 dB
	90°	3632	-47.80 dB	1536	42.29%	19.34 dB
	180°	3663	-47.84 dB	999	27.27%	19.17 dB
	270°	3688	-47.87 dB	780	21.15%	17.15 dB
UMi (30 km $\times$ 30 km)	No Protection	21,193	-55.46 dB	12,218	57.65%	27.78 dB
	45°	22,277	-55.68 dB	12,394	55.64%	27.01 dB
	90°	22,539	-55.73 dB	11,586	51.40%	25.12 dB
	180°	22,622	-55.74 dB	7400	32.71%	24.91 dB
	270°	22,699	-55.74 dB	5870	25.86%	22.79 dB

Table 5. Mean transmission (Tx) power reduction in the restriction zone for RMa, UMa, and UMi using a 16×16 antenna array.

Region Type	Beam Shut-Off Range	No. of Deployable Base Stations	Restriction Zone Interference Threshold	No. of Restriction Zone Base Stations	% of Deployed Base Stations Requiring Tx Power Control	Mean Tx Power Reduction in Restriction Zone
RMa ($100 \text{ km} \times 100 \text{ km}$)	No Protection	3194	−47.24 dB	886	27.74%	17.51 dB
	45°	3331	−47.43 dB	676	20.29%	14.49 dB
	90°	3345	−47.44 dB	493	14.74%	13.09 dB
	180°	3352	−47.45 dB	351	10.47%	12.26 dB
	270°	3358	−47.46 dB	259	7.71%	10.15 dB
UMa ($30 \text{ km} \times 30 \text{ km}$)	No Protection	3300	−47.39 dB	1749	53.00%	21.07 dB
	45°	3622	−47.79 dB	1623	44.81%	19.29 dB
	90°	3666	−47.84 dB	1159	31.61%	18.41 dB
	180°	3688	−47.87 dB	809	21.94%	18.39 dB
	270°	3697	−47.88 dB	623	16.85%	14.92 dB
UMi ($30 \text{ km} \times 30 \text{ km}$)	No Protection	20,855	−55.39 dB	13,010	62.38%	28.35 dB
	45°	22,492	−55.72 dB	12,201	54.24%	25.55 dB
	90°	22,646	−55.75 dB	9683	42.76%	24.08 dB
	180°	22,692	−55.76 dB	6223	27.42%	23.89 dB
	270°	22,746	−55.77 dB	4886	21.48%	21.50 dB

These tables reveal that a higher beam shut-off range results in lower BS interference, leading to a smaller exclusion zone. Then, the total number of BSs that can be deployed increases. The interference threshold for the restriction zone slightly changes when the beam shut-off range increases. The number of BSs in the restriction zone continues to decrease when the protection level increases. The percentage of deployed BSs requiring Tx power control also decreases when the beam shut-off range increases. The mean Tx power reduction in the restriction zone first increases when using the 45° beam shut-off range compared with when angular protection does not exist. The power decreases when the level of angular protection increases. When using the same beam shut-off angle, the exclusion zones of the 8×8 and 16×16 arrays become smaller than that of the 4×4 array. Therefore, the total number of BSs that can be deployed increases. In addition, when using the same 45° and 90° beam shut-off angles, the 8×8 array has the highest percentage of deployed BSs that require Tx power control. However, when using 180° and 270° beam shut-off angles, the antenna array with the largest number of elements has the lowest percentage of deployed BSs that require Tx power control. With the same beam shut-off angle, the 4×4 and 8×8 antenna arrays have a very similar mean Tx power reduction in the restriction zone. The 16×16 antenna array has the lowest mean Tx power reduction in the restriction zone. Therefore, in UMi, the most efficient angular protection in terms of the number of deployable BSs and the power reduction is achieved using a 16×16 antenna array.

5. Conclusions

In this study, a new angular isolation method was proposed to enable the coexistence of the FSS ESs and BSs. This method solves the influence of the ES antenna elevation angle on the protection method. Further, the methods of determining the area and power control scheme within the restricted area were verified.

The numerical results reveal that, when combining distance protection and angular protection, both the exclusion and restriction zones can be decreased at the expense of the beam sweep angle of the BSs using angular protection. In addition, a higher beam shut-off range (i.e., sacrificing more beam sweep angles) leads to smaller exclusion and restriction zones. A tradeoff exists between the coexistence of beam sweep angles of BSs. As the number of antenna elements increases, the angular protection becomes more efficient.

Moreover, the advantage of beamforming the antenna arrays is more significant in UMa and UMi than in RMa. In UMa and UMi, only minor improvements of the exclusion zone can be achieved when using 90°, 180° and 270° beam shut-off ranges compared with using a 45° beam shut-off range. In contrast to the exclusion zone, the size of the restriction zone significantly decreases as the beam shut-off range increases to 90°, 180° and 270°. As for UMa and UMi, angular protection is primarily efficient in terms of the number of deployable BSs and the power control efficiency when using an antenna array with a high number of elements. The proposed method can help in the actual 5G network design and deployment when dealing with the coexistence of the 5G system and the satellite system. The exclusion and restriction zones can be achieved by loading the actual parameters of the ES and 5G BSs. Consequently, cases in which no BSs can exist and where BSs can be deployed are differentiated. With the proposed power control scheme, the maximum Tx power of each BS in the restriction zone can be achieved either using the 3GPP network layout or by customizing the BS site selection.

In future work, we expect to focus on developing guard band protection measures to mitigate the interfering beams, decrease the size of the exclusion and restriction zones, and decrease the BS Tx power within the restriction zone. Finally, hybrid technologies can also be considered in future generation systems, such as 6G, because nonterrestrial networks will become part of it.

Author Contributions: Y.W. and S.-H.H. contributed to the main idea of this research work. Y.W. and S.L. wrote the computation codes and performed the simulations, experiments, and database collection. Y.W., S.L. and S.-H.H. confirmed the numerical results of the work. The research activity was planned and executed under the supervision of S.-H.H. In addition, S.L., Y.W. and S.-H.H. contributed to the writing of this article. All authors have read and agreed to the published version of the manuscript.

Conflicts of Interest: The authors declare no conflict of interest.

References

1. Anisimoff. 5G Bands in South Korea. Available online: http://anisimoff.org/eng/5g/spectrum/5g_south_korea.html (accessed on 13 May 2021).
2. Hattab, G.; Moorut, P.; Visotsky, E.; Cudak, M.; Ghosh, A. Interference Analysis of the Coexistence of 5G Cellular Networks with Satellite Earth Stations in 3.7–4.2 GHz. In Proceedings of the 2018 IEEE International Conference on Communications Workshops (ICC Workshops), Kansas City, MO, USA, 20–24 May 2018; Institute of Electrical and Electronics Engineers (IEEE): Piscataway, NJ, USA, 2018; pp. 1–6.
3. Guidolin, F.; Nekovee, M.; Badia, L.; Zorzi, M. *A Study on the Coexistence of Fixed Satellite Service and Cellular Networks in a mmWave Scenario*; Institute of Electrical and Electronics Engineers (IEEE): Piscataway, NJ, USA, 2015; pp. 2444–2449.
4. ITU Radio Regulations, Section IV. Radio Stations and Systems. Available online: https://www.itu.int/dms_pub/itu-r/md/15/wrs18/sp/R15-WRS18-SP-0003!!PDF-E.pdf (accessed on 13 May 2021).
5. ETRI Metis Project. Intermediate Description of the Spectrum Needs and Usage Principles. D5.1 Deliverable, August 2013. Available online: https://metis2020.com/wp-content/uploads/deliverables/METIS_D5.1_v1.pdf (accessed on 13 May 2021).
6. Wei, Y.; Liu, S.; Hwang, S.-H. Distance protection for coexistence of 5G base station and satellite Earth station. *Electronics* **2021**, *10*, 1481. [CrossRef]
7. Son, H.-K.; Chong, Y.-J. Coexistence of 5G system with Fixed satellite service Earth station in the 3.8 GHz Band. In Proceedings of the 2018 International Conference on Information and Communication Technology Convergence (ICTC), Jeju, Korea, 17–19 October 2018; pp. 1070–1073.
8. Park, Y.G.; Lee, I.K. Impact of 5G New Radio Downlink Signal on Fixed-Satellite Service Earth Station. *J. Inf. Commun. Converg. Eng.* **2020**, *18*, 155–161.
9. Castellanos, G.; Teuta, G.; Penagos, H.P.; Joseph, W. Coexistence for LTE-Advanced and FSS Services in the 3.5 GHz Band in Colombia. In Proceedings of the 2020 10th Advanced Satellite Multimedia Systems Conference and the 16th Signal Processing for Space Communications Workshop (ASMS/SPSC), Graz, Austria, 20–21 October 2020; pp. 1–7.
10. Guidolin, F.; Nekovee, M. Investigating Spectrum Sharing Between 5G Millimeter Wave Networks and Fixed Satellite Systems. In Proceedings of the 2015 IEEE Globecom Workshops (GC Wkshps), San Diego, CA, USA, 6–10 December 2015; pp. 1–7.

11. CEPT ECC Report 254. Operational Guidelines for Spectrum Sharing to Support the Implementation of the Current ECC Framework in the 3600–3800 MHz Range. Available online: https://docdb.cept.org/document/958 (accessed on 13 May 2021).

12. Sun, Q.; Nan, S. Coexistence Studies between LTE-Hotspot Indoor and Earth Station of Fixed Satellite Service in the Band 34003600MHz. In Proceedings of the 2012 IEEE 11th International Conference on Signal Processing, Beijing, China, 21–25 October 2012; Volume 3, pp. 2275–2278.

13. Kim, S.; Visotsky, E.; Moorut, P.; Bechta, K.; Ghosh, A.; Dietrich, C. Coexistence of 5G with the incumbents in the 28 and 70 GHz bands. *IEEE J. Sel. Areas Commun.* **2017**, *35*, 1254–1268. [CrossRef]

14. Karimi, H.R.; Casagni, A.; Gulyaev, A. Spectrum Sharing Between the Mobile Service and Existing Fixed and Fixed Satellite Services in the 3.6–3.8 GHz Band. In Proceedings of the 2015 IEEE International Symposium on Dynamic Spectrum Access Networks (DySPAN), Stockholm, Sweden, 29 September–2 October 2015; pp. 142–153.

15. ITU-R Report S.2368-0. Sharing Studies between International Mobile Telecommunication-Advanced Systems and Geostationary Satellite Networks in the Fixed-Satellite Service in the 3400–4200 MHz and 4500–4800 MHz Frequency Bands in the WRC Study Cycle Leading to WRC-15. 2015. Available online: https://www.itu.int/pub/R-REP-S.2368 (accessed on 13 May 2021).

16. 3GPP. Study on Channel Model for Frequencies from 0.5 to 100 GHz (Release 15). 3GPP TR 38.901 V15.0.0. 2018. Available online: https://www.etsi.org/deliver/etsi_tr/138900_138999/138901/14.00.00_60/tr_138901v140000p.pdf (accessed on 13 May 2021).

17. ITU-R P.452-15. Prediction Procedure for the Evaluation of Interference between Stations on the Surface of the Earth at Frequencies above about 0.1 GHz. 2013. Available online: https://www.itu.int/rec/R-REC-P.452/en (accessed on 13 May 2021).

18. 3GPP. Radio Frequency (RF) System Scenarios (Release 15). 3GPP TR 36.942 V15.0.0. 2018. Available online: https://portal.3gpp.org/desktopmodules/Specifications/SpecificationDetails.aspx?specificationId=2592 (accessed on 13 May 2021).

19. 3GPP. Evolved Universal Terrestrial Radio Access (E-UTRA): Base Station (BS) Radio Transmission and Reception (Release 15). 3GPP TS 36.104 V15.0.0. 2018. Available online: https://portal.3gpp.org/desktopmodules/Specifications/SpecificationDetails.aspx?specificationId=2412 (accessed on 13 May 2021).

20. 3GPP. NR: Base Station (BS) Radio Transmission and Reception (Release 15). 3GPP TS 38.104 V15.3.0. 2018. Available online: https://www.lp-ats.com/smart-pcb-stacking?https://www.lp-ats.com/smart-pcb-stacking%3Futm_source%3DGoogle%26utm_medium%3Dads%26utm_campaign%3D12766553251%26utm_term%3D515054125127&gclid=EAIaIQobChMI-cXkj42e8QIVA3ZgCh05XQiKEAAYASAAEgKc-PD_BwE (accessed on 13 May 2021).

21. 3GPP. Study of Radio Frequency (RF) and Electromagnetic Compatibility (EMC) Requirements for Active Antenna Array Sys-tem (AAAS) Base Station (Release 12). 3GPP TR 37.840 V12.1.0. 2013. Available online: https://www.mvg-world.com/en/products/emc/emc-antennas/emc-dual-ridge-horn-antenna-eh022?gclid=EAIaIQobChMI8KaWro2e8QIVhnZgCh1cnQN8EAAYASAAEgKuCvD_BwE (accessed on 13 May 2021).

22. ITU-R S.465-6. Reference Radiaton Pattern for Earth Station Antennas in the Fixed-Satellite Service for Use in Coordination and Interference Assessment in the Frequency Range from 2 to 31 GHz. 2010. Available online: https://www.itu.int/rec/R-REC-S.465/_page.print (accessed on 18 January 2022).